Nanoscale

PAPER

View Article Online
View Journal | View Issue

Cite this: *Nanoscale*, 2025, **17**, 4765

Simultaneous pore confinement and sidewall modification of an N-rich COF with Pd(II): an efficient and sustainable heterogeneous catalyst for cross-coupling reactions†

Atikur Hassan, ‡ Ayush Kumar, ‡ Sk Abdul Wahed, Subhadip Mondal, Amit Kumar * and Neeladri Das *

Covalent organic frameworks (COFs) are crystalline porous materials bearing well-ordered two- or three-dimensional molecular tectons in their polymeric skeletal framework. COFs are structurally robust as well as physiochemically stable. Currently, these are being developed for their use as "heterogeneous catalysts" for various organic transformations. In particular, research on the use of COFs for catalysis for different C–C cross-coupling reactions is in its infancy. To date, COF catalysts reported for such reactions bear Pd (II) bound in an exclusive coordination environment and have been explored for a particular organic reaction. Herein, we report, for the first time, a COF (Pd@COF-TFP_TzPy) that can anchor Pd(II) units in the polymeric framework in two different coordination environments. Thus, Pd@COF-TFP_TzPy is a porous material with a dual confinement environment for Pd(II) units. The precursor COF (COF-TFP_TzPy) was easily synthesized and it features a two-dimensional hexagonal sheet structure for facile incorporation of Pd(II) ions. The loading of Pd(II) into Pd@COF-TFP_TzPy was low (4.85 wt% Pd), yet the material exhibited excellent catalytic activity in diverse C–C cross-coupling reactions with a broad substrate scope. Furthermore, Pd@COF-TFP_TzPy is highly stable and recyclable, thereby ensuring sustainable utilization of expensive Pd metal. We anticipate that our approach will stimulate further research into designing and utilizing functional COF materials for catalysis.

Received 15th September 2024,
Accepted 7th January 2025

DOI: 10.1039/d4nr03796k

rsc.li/nanoscale

Introduction

Carbon–carbon bonds are fundamental and ubiquitously present in many natural and synthetic organic molecules, either in cyclic or acyclic frameworks.[1] Consequently, constructing these bonds is one of the most challenging and important tasks for organic chemists. Transition-metal-catalyzed cross-coupling is a cornerstone synthetic tool in modern science for forming Csp^2–Csp and Csp^2–Csp^2 bonds. Due to their broad applications and ease of use, cross-coupling strategies are widely utilized in the preparation of high value-added molecules such as active pharmaceutical ingredients, functional materials, and agrochemicals *via* the introduction of desired carbon–carbon bonds. Nonetheless, these reactions have become essential in the daily practice of synthetic chemists. Among the most important cross-coupling reactions for forming Csp^2–Csp^2 or Csp^2–Csp bonds are the Suzuki–Miyaura cross-coupling (SMCC), Mizoroki–Heck cross-coupling (MHCC) and Sonogashira cross-coupling (SCC) reactions.[2–5] Traditionally, these reactions are catalyzed by homogeneous Pd salts in the presence of ligands such as phosphines and N-heterocyclic carbenes (NHCs), which facilitate the formation of required C–C, C=C, and C≡C bonds, respectively.[6,7] While homogeneous Pd catalysts offer several advantages, they also come with significant disadvantages. These include multi-step preparation, the use of toxic solvents and ligands, and the presence of Pd complex residues in the reaction media.[8] To develop more economical and sustainable processes, recycling expensive Pd catalysts is essential.[9] Additionally, removing moisture-sensitive ligands from the products using chromatography, distillation, and extraction techniques remains difficult.[10,11] Hence, designing sustainable catalytic strategies for desired C–C bond formation, such as heterogeneous catalytic approaches using inexpensive substrates with simple cata-

Department of Chemistry, Indian Institute of Technology Patna, Patna 801106, Bihar, India. E-mail: amitkt@iitp.ac.in, neeladri@iitp.ac.in, neeladri2002@yahoo.co.in

†Electronic supplementary information (ESI) available: Synthesis of COF-TFP_TzPy and Pd@COF-TFP_TzPy and the monomers, general characterization of COF-TFP_TzPy and Pd@COF-TFP_TzPy, general procedures for the coupling reaction, comparison table, and NMR spectra of the synthesized compounds. See DOI: https://doi.org/10.1039/d4nr03796k

‡The authors contributed equally to this work.

lytic systems, is a highly desirable and ongoing goal in contemporary organic synthesis.[12] This approach can address the aforementioned issues effectively.

One possible approach in the quest to obtain a useful heterogeneous catalyst for cross-coupling reactions is to immobilize palladium on insoluble support matrices.[13–15] This strategy offers several advantages, including improved catalyst stability, facile separation and purification of products, and increased reusability of the expensive metal catalyst.[16] Consequently, several methods have been developed to prepare stable and effective heterogeneous Pd catalysts for promoting these important cross-coupling reactions *via* green chemical pathways, which are desirable from both sustainable and economic perspectives. Over the last decade, many scientists have immobilized Pd on different solid supports to combine the advantages of homogeneous and heterogeneous catalysts. These catalysts can be recovered by filtration or centrifugation, avoiding the traditional challenges of catalyst separation and reuse. Commercially available Pd/C and Pd/Al_2O_3 could be alternatives to homogeneous Pd catalysts, but the leaching of palladium, aggregation, and low efficacy make them less suitable in many cases.[17] Also, the use of heterogeneous Pd catalysts has introduced new problems such as low activity and selectivity, the need for stringent reaction conditions, increased by-product formation and leaching of metal species.[11] Moreover, heterogeneous catalysts need harsher reaction conditions in comparison with homogeneous catalysts. Therefore, research continues to develop effective heterogeneous catalysts with superior practical properties to overcome these drawbacks.

Many new solid-supported palladium catalysts have been designed during the last few decades based on activated carbon, inorganic oxides, metal–organic frameworks (MOFs), silica nanoparticles, porous organic polymers (POPs), *etc.*, to improve the catalytic activity and stability of Pd.[18] However, the high catalyst loading and non-uniform nature limit their application in an energy economical manner. An efficient solid-supported metal catalyst features a uniform dispersion of the active metal (such as palladium).[19–21]

Metal aggregation can be easily avoided by the grafting of chelating groups such as phosphine ligands and amine groups or by the incorporation of heteroatoms such as nitrogen, sulphur, and phosphorus, which bind with the metal sites and ensure their uniform distribution.[22,23] Overall, due to changes in the chemical and electrical properties of the immobilized metal center, its interaction with the substrate molecules is expected to improve.

In this regard, covalent organic frameworks (COFs) are an emerging class of porous crystalline materials constructed from molecular building blocks *via* covalent bonds, making them an ideal choice for immobilization of Pd.[19,24–26] These materials have garnered significant interest due to their remarkable properties, including π-conjugated skeletons, high surface areas, and customizable functions.[27–30] The flexible design and modular synthesis of COFs endow them with great potential in various applications, such as catalysis, optoelectronics, sensing, biomedicine, energy storage, separation, and environmental remediation.[31–37] COF synthesis is governed by dynamic covalent chemistry, which allows for the formation of well-ordered network structures through error correction.[38–40] Crystallinity is a crucial feature in the development of novel COFs, as the quality of COF crystals significantly influences the physiochemical properties of the resulting materials.[41,42] Due to the strong covalent bonds, the abundance of heteroatoms, and the possibility for highly tuneable structures, COFs are highly promising materials for the immobilization of metals.[19,39,43–46] The main important factors that should be considered for COFs as solid supports are their thermal stability and resistance in aqueous acidic and basic solvents. From this point of view, imine COFs have been explored due to their good stability in various media and their ease of functionalization for practical applications.[20,39] In recent literature, there are only a handful of reports describing the immobilization of Pd on covalent organic frameworks (COFs).[47] The resulting heterogeneous catalysts are interesting materials due to their inherent and desirable characteristics such as high surface areas, physiochemical and thermal stabilities, tailorable catalytic properties and versatile nature. Among the COFs, the one that contains imine linkages is most popular, wherein the Pd center can be efficiently anchored on the COF *via* coordination with the imine Nitrogen centers. For example, Pd was bound to COF-LZU-1 and Pd/H_2P-Bph-COF to obtain efficient heterogeneous catalysts that are specific for the Suzuki cross coupling reaction.[40,48] There are four methods for using COFs as catalysts.[19,49] Among these, sidewall modification and pore confinement are the most commonly used techniques for immobilising metal ions.[19] These techniques are illustrated in Fig. 1; Fig. 1a shows pore confinement, while Fig. 1b shows sidewall modification.[40,50] This gap in the literature inspired us to design a COF with multiple interaction sites for palladium coordination. Our aim was to develop a COF material with enhanced catalytic properties by incorporating multiple coordination sites for Pd, thereby improving its versatility for various cross-coupling reactions. In this regard, we have synthesized a nitrogen-rich COF (COF-TFP_TzPy) that has a high surface area with multiple coordination sites for palladium. The as-obtained COF was characterized with various techniques. The Pd-loaded COF (Pd@COF-TFP_TzPy) was also well characterized. Pd@COF-TFP_TzPy was simultaneously employed as a heterogeneous catalyst for the Suzuki, Heck and Sonogashira cross-coupling reactions and in each case, efficient C–C bond formation was recorded between the two coupling reactant molecules. The experimental details and associated results are discussed elaborately in the upcoming sections.

Results and discussion

The arene monomer (TFP) with three aldehyde groups was obtained using the Duff reaction, while the amine monomer

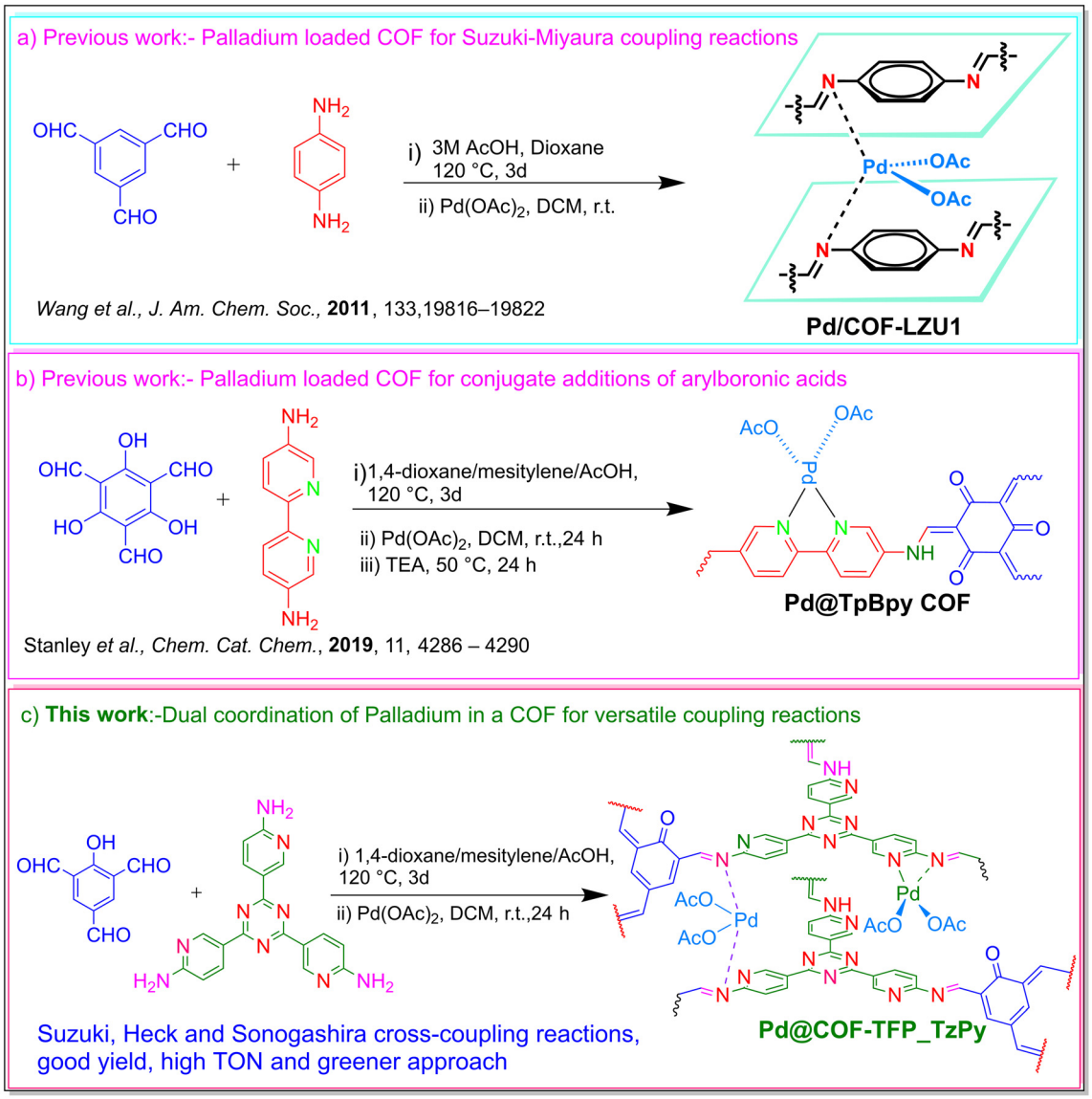

Fig. 1 (a and b) Different modes of Pd coordination in a COF. (c) Dual mode of the coordination of Pd in a single COF.

(Tz-Py) was obtained *via* a one-step cyclotrimerization reaction (details are provided in ESI pages S4 and S5†).[51,52] Subsequently, a covalent organic framework (COF-TFP_TzPy) was obtained through the Schiff-base polycondensation reaction using the above-mentioned monomers under solvothermal conditions (Scheme 1).[52,53] The product obtained was washed with organic solvents (such as THF, DMF, and methanol) and dried at 120 °C to obtain the final desired product as a red-coloured powdery material. The detailed synthesis procedures of COF-TFP_TzPy and Pd@COF-TFP_TzPy are included in Scheme 1 and the ESI (pages S5 and S6†). The obtained materials (COF-TFP_TzPy and Pd@COF-TFP_TzPy) were thoroughly characterized to support their formation.

The Fourier Transform Infrared (FT-IR) spectrum of the as-synthesised COF-TFP_TzPy showed a peak at 1608 cm^{-1} that was attributed to the newly formed C=N bond (Fig. 2a). The bands corresponding to C=O at 1674 cm^{-1} present in the TFP monomer were absent in the IR spectrum of COF-TFP_TzPy. Also, the absence of the band at ~3300 cm^{-1} due to $-NH_2$ that was observed in TzPy, clearly indicated the completion of the condensation reaction *via* the formation of imine linkages. After loading COF-TFP_TzPy with Pd, the imine bond shifted slightly due to their expected coordination with palladium. In addition, the C–N bond vibration was blue-shifted to 1286 cm^{-1}, further indicating the interaction of Pd with the pyridine nitrogen.[27]

The yield of COF-TFP_TzPy *via* imine linkages was eventually verified by recording its solid-state ^{13}C NMR spectrum (Fig. 2b). The formation of the imine-linked structure was confirmed due to the appearance of the signal at 159.9 ppm that was assigned to the carbon of the C=N imine bond. A peak with a chemical shift at 170 ppm indicated the incorporation

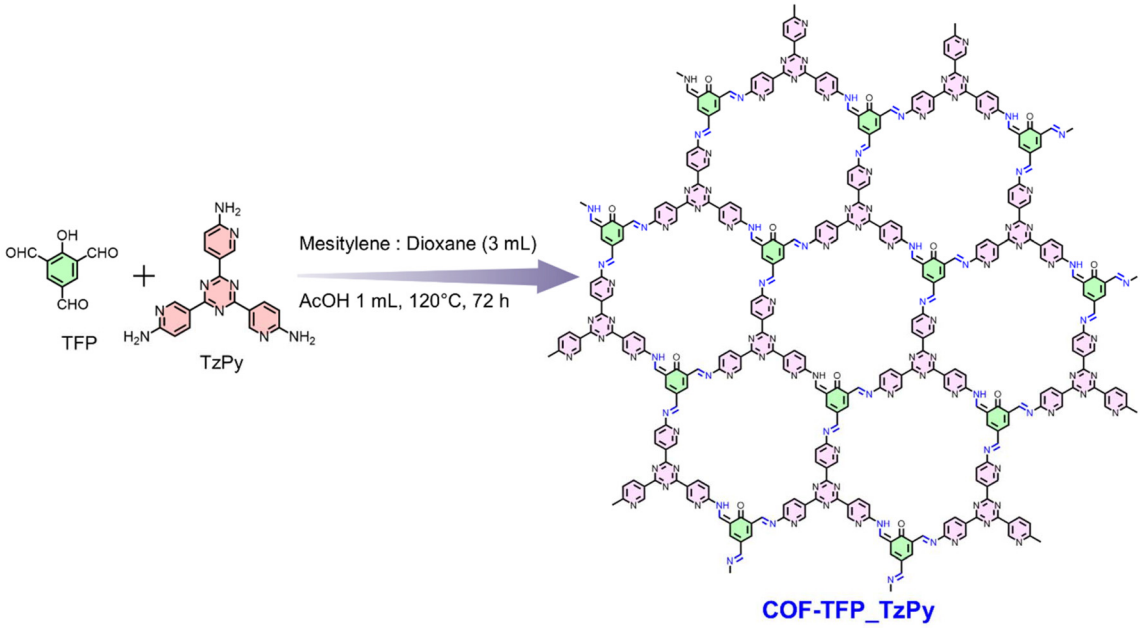

Scheme 1 Synthesis of COF-TFP_TzPy.

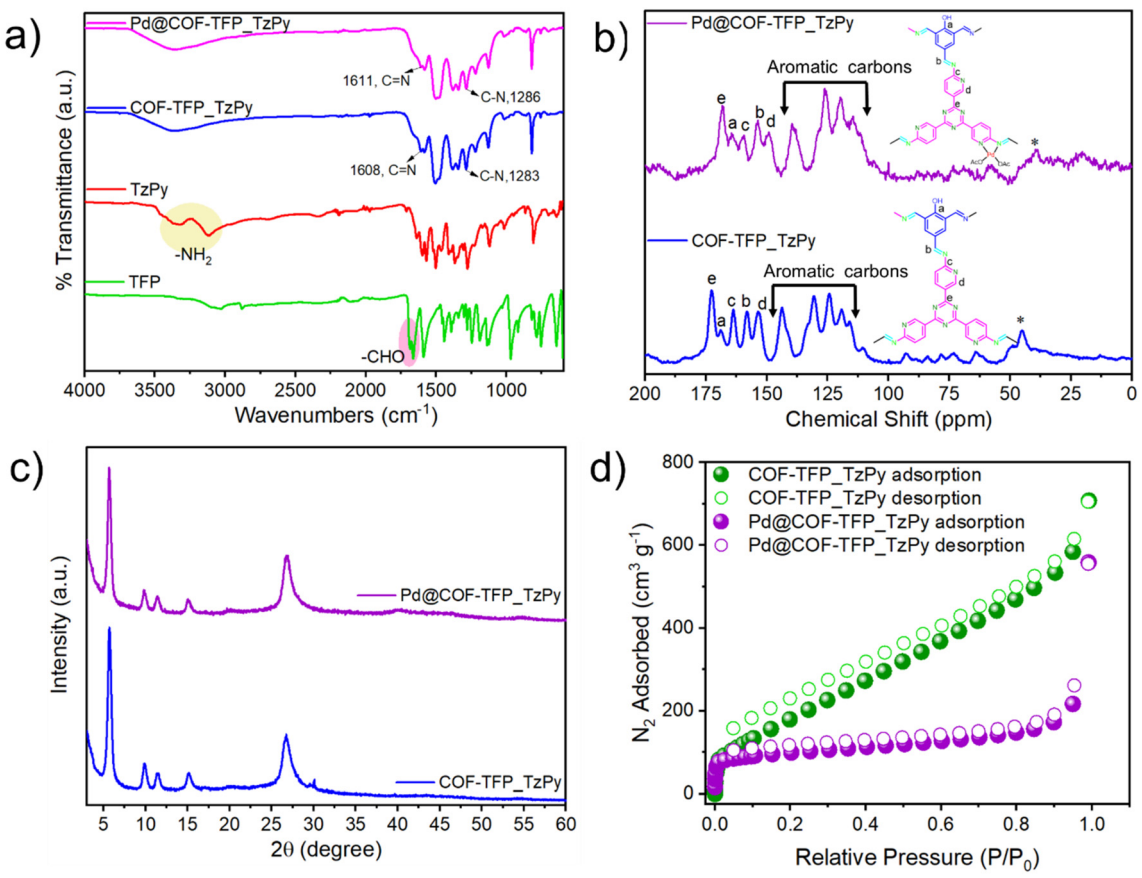

Fig. 2 (a) FT-IR spectra of COF-TFP_TzPy and Pd@COF-TFP_TzPy. (b) Solid-state ^{13}C-NMR spectra of COF-TFP_TzPy and Pd@COF-TFP_TzPy (* indicates side bands). (c) Powder X-ray diffraction patterns of COF-TFP_TzPy and Pd@COF-TFP_TzPy. (d) Low-temperature N_2 adsorption–desorption isotherm.

of the triazine ring, while the aromatic carbons originating from the TFP monomer appeared in between 120 and 145 ppm. After loading Pd into the COF-TFP_TzPy network, slight changes were observed in the chemical shift of various carbon atoms present in the ^{13}C NMR spectrum of Pd@COF-TFP_TzPy. The corresponding ^{13}C NMR spectrum with complete peak assignment of the carbon atoms is shown in Fig. 2b. These results effectively verify the formation of the imine-linked COF with respect to the chemical composition and structure shown in Scheme 1. The crystallinity of COF-TFP_TzPy and Pd@COF-TFP_TzPy was investigated by powder X-ray diffraction (PXRD) experiments. COF-TFP_TzPy exhibited a series of intense diffraction peaks (Fig. 2c), indicating the presence of long-range ordering in this material. Specifically, a sharp and intense peak was observed at 5.68° along with other small peaks at 9.48, 11.45, 15.15 and 26.7° corresponding to reflections from the (100), (110), (200), (120) and (001) planes, respectively.[52,53] The PXRD of Pd@COF-TFP_TzPy also showed almost the same intense diffraction peaks, indicating its highly crystalline nature. The thermal behaviours of COF-TFP_TzPy and Pd@COF-TFP_TzPy were studied by subjecting their pristine samples to thermogravimetric analysis (TGA). In both cases, upon heating a sample under a nitrogen atmosphere, the TGA thermogram showed a weight loss of approximately 30% and 60% at 400 °C and 800 °C, respectively. These data suggested that COF-TFP_TzPy and Pd@COF-TFP_TzPy have good thermal stability (Fig. S1†). The presence of the permanent porosity of the COF-TFP_TzPy and Pd@COF-TFP_TzPy COFs was verified by N_2 sorption measurements at 77 K. Both COFs exhibited type II isotherms with a sharp increase at low pressure ($P/P_0 < 0.05$), indicating their microporous nature (Fig. 2d). The Brunauer–Emmett–Teller (BET) surface areas were calculated to be 770 $m^2\ g^{-1}$ and 360 $m^2\ g^{-1}$, respectively, for COF-TFP_TzPy and Pd@COF-TFP_TzPy (Fig. S2 and S3†). Pore size distribution analysis using the Density Functional Theory (DFT) method suggested the presence of narrow micropores of size less than 1 nm (Fig. S4 and S5†). A good carbon dioxide uptake at two different temperatures was recorded by COF-TFP_TzPy and Pd@COF-TFP_TzPy (Fig. S6†). A significant decrease in the surface area of Pd@COF-TFP_TzPy was expected since Pd(II) units are coordinated with the available N-centers on the surface and pores of COF-TFP_TzPy. In other words, upon immobilisation of $Pd(OAc)_2$ on COF-TFP_TzPy, the surface area of the COF decreased due to the partial blocking of the pores by the Pd centers. Thus, the low-temperature gas sorption analysis also indicated the successful coordination of Pd with ample nitrogen-based ligating centers in the skeleton of the COF.

The morphologies associated with COF-TFP_TzPy and Pd@COF-TFP_TzPy were studied using Field Emission Scanning Electron Microscopy (FE-SEM) and High-Resolution Transmission Electron Microscopy (HR-TEM) techniques. COF-TFP_TzPy showed the formation of hexagonal flake-stacked microstructures in its FE-SEM micrograph (Fig. S7†). Such a morphology was retained in the case of Pd@COF-TFP_TzPy (Fig. 3a–c). Furthermore, EDX mapping analysis indicates the presence of Pd in Pd@COF-TFP_TzPy, while that of pristine COF-TFP_TzPy showed the presence of only C, N and O atoms (Fig. 3d and Fig. S8–S10†).

The hexagonal flake-shaped morphologies associated with COF-TFP_TzPy and Pd@COF-TFP_TzPy were also evident from their corresponding TEM images (Fig. 4 and Fig. S11†). In the case of Pd@COF-TFP_TzPy, Pd was well dispersed in the matrix of the COF. Black spots in the images represent Pd particles (Fig. 4a–f). The HR-TEM image (Fig. 4f) suggests that the dimension of the catalytic center is within 5 nm. The XPS analysis of COF-TFP_TzPy and Pd@COF-TFP_TzPy showed the presence of the expected elements in the respective survey spectra (Fig. 5a and Fig. S12†).

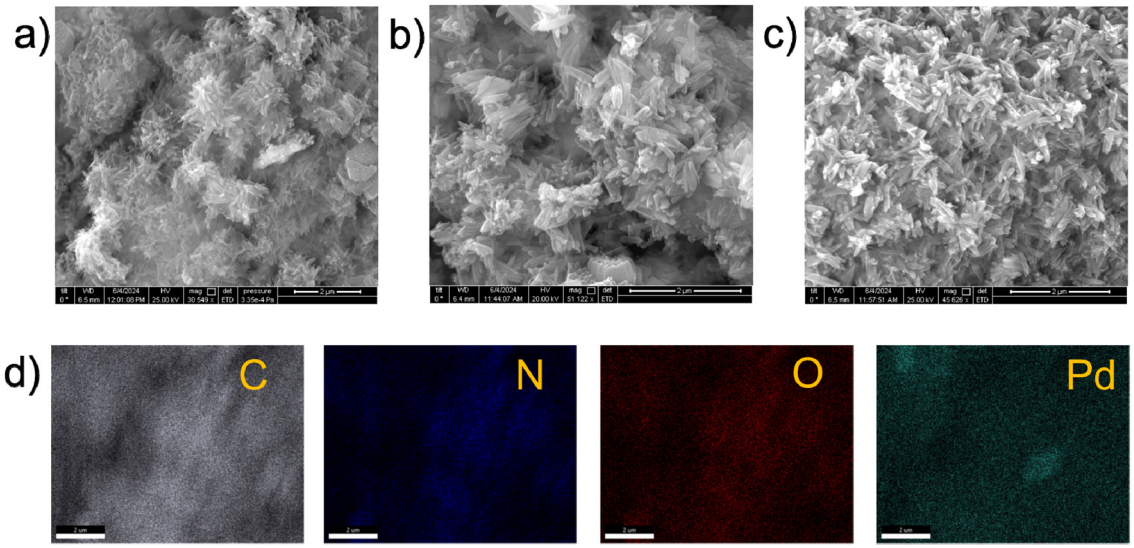

Fig. 3 (a–c) FE-SEM images of Pd@COF-TFP_TzPy. (d) EDX mapping of Pd@COF-TFP_TzPy.

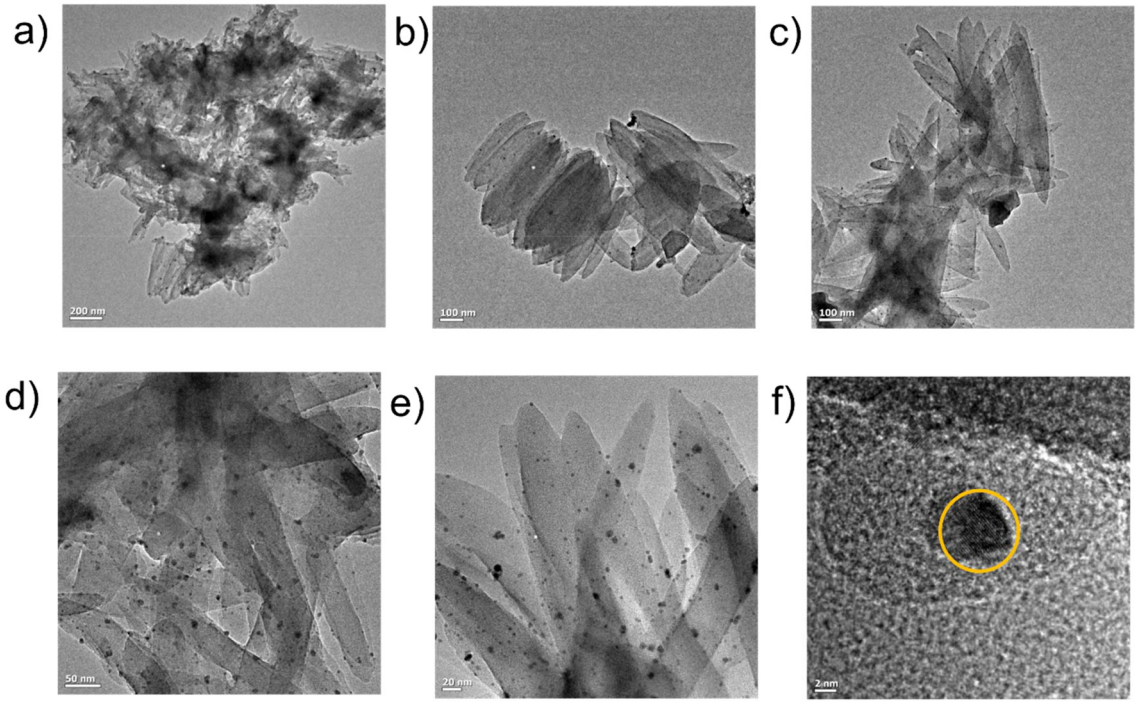

Fig. 4 (a–c) TEM images of Pd@COF-TFP_TzPy. (d–f) HR-TEM images of Pd@COF-TFP_TzPy.

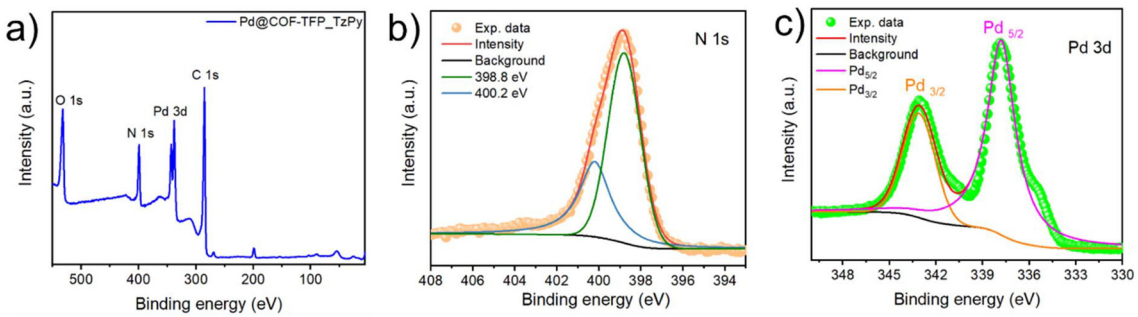

Fig. 5 (a) XPS survey spectra of Pd@COF-TFP_TzPy. (b) HR-XPS of the N 1s spectrum. (c) HR-XPS of Pd 3d in Pd@COF-TFP_TzPy.

The deconvoluted N 1s XPS spectra of COF-TFP_TzPy showed peaks at ~398.7 and ~400.1 eV, corresponding to the nitrogen in the –C═N bond (from imine, pyridine, and triazine groups) and the secondary amine nitrogen, respectively (Fig. S12b†).[53] Furthermore, after binding to Pd, the deconvoluted N 1s XPS spectra of the COF showed peaks at around 398.8–400.2 eV, which shifted slightly to higher binding energies, indicating coordination with Pd (Fig. 5b). Additionally, the Pd 3d HR-XPS spectral data of a sample of Pd@COF-TFP_TzPy showed the presence of two peaks centered at 337.8 and 343.1 eV that were assigned to Pd(II) $3d_{5/2}$ and $3d_{3/2}$ orbitals, respectively (Fig. 5c).[15,40,54–56] These signals confirm the presence of Pd(II) species in Pd@COF-TFP_TzPy. Also, the binding energy of $3d_{3/2}$ in the range of 333–345 eV has been attributed previously by others to Pd in the +2 oxidation state.[15,40,57] The mode of coordination of the nitrogen with both the pyridine and amine moieties has also been well-reported in the literature.[18,58–60] Minimal metal loading, as measured by ICP-AES analysis, indicated the superior stability of Pd@COF-TFP_TzPy in which the Pd content was 4.85 wt%. The low Pd loading can be a desirable aspect as the catalytic material would be cost-effective and sustainable from economic and environmental perspectives. In addition, the good crystallinity and stability of Pd@COF-TFP_TzPy ensure that the Pd-loaded COF meets the requirements expected for a material with potential applications in the domain of heterogeneous catalysis. Therefore, Pd@COF-TFP_TzPy was explored as a catalyst for various Pd(II)-catalyzed cross-coupling reactions, where palladium can be used in a sustainable and eco-friendly manner. The chemical stability of the COF was evaluated by immersion in 1 M HCl and 1 M NaOH. After immersion, the COF was air dried and its PXRD and FT-IR spectra were

recorded (Fig. S13†). The data indicate that the COF remains stable in both acidic and basic aqueous media.

To demonstrate the synthetic application of our newly developed Pd@COF-TFP_TzPy catalyst for the Suzuki–Miyaura cross-coupling (SMCC) reaction, we began by investigating the reaction between 4-iodotoluene (**1a**) and phenylboronic acid (**2a**), as detailed in Table 1. Initially, when a mixture of 1.0 equiv. of **1a** and 1.5 equiv. of **2a** was treated with 5 mg (0.56 mol%) of Pd@COF-TFP_TzPy catalyst and K_3PO_4 as a base in an EtOH solvent at room temperature, the desired product **3a** was obtained with an 83% yield (entry 1). Building on this promising result, we conducted a comprehensive survey of reaction conditions, including solvent, base, and reaction time, to optimize the yield of the desired product.

The base plays a crucial role in the SMCC reaction by converting phenylboronic acid into the more reactive phenyl-organoboronate, thus enhancing the rate of the transmetallation step. We explored various bases, including K_3PO_4, K_2CO_3, and NaOH, for reaction optimization (entries 1–3). Among these, NaOH provided the highest yield. Using ethanol alone as the solvent resulted in a poor yield (entry 4), while no reaction occurred in water (entry 5). Therefore, we employed a biphasic solvent system of ethanol and water (1 : 1), which effectively dissolved both organic compounds and inorganic catalysts. Further solvent screening confirmed that the ethanol and water mixture was the most suitable. To highlight the superiority of our Pd@COF-TFP_TzPy catalyst, we conducted a reaction under similar conditions using Pd/C as a catalyst, which yielded only 62% (entry 11). After thorough optimization, the reaction conditions described in entry 2 were identified as the best.

With the optimized reaction conditions in hand, we further explored the substrate scope for both coupling partners (aryl halide and aryl boronic acid, Scheme 2). First, we examined the substrate scope with respect to aryl iodides either with electron-withdrawing or electron-donating groups, affording the desired SMCC products (**3a–3j**) in yields ranging from 79% to 94%. We further diversified our investigation by varying phenylboronic acids, which resulted in good to excellent yields (**3k–3u**, 71%–96%). Bulky naphthyl substrates also performed excellently under the optimized conditions (**3t–3u**, 95%–97%). Additionally, we extended the substrate scope to include heterocyclic scaffolds under the optimized reaction conditions. Reactions with thiophene yielded heterocycle-coupled biaryl products (**3s**, 71%). The reaction of 1-bromo-4-iodobenzene with phenylboronic acid produced two coupling products: 4-bromo-1,1′-biphenyl and 1,1′:4′, 1′-terphenyl (**3y and 3y′**, 71% and 25%, respectively). Similar outcomes were observed for the reaction of phenylboronic acid with 1-bromo-2-iodobenzene and the reaction of iodobenzene with (4-bromophenyl)boronic acid (**3z–3aa′**). To further diversify our investigation, aryl bromides as coupling partners were reacted with differentially substituted boronic acids under similar conditions, yielding the desired cross-coupled products (**3ab–3ae**, 81%–94%). This study demonstrates that the designed heterogeneous catalyst (Pd@COF-TFP_TzPy) is highly effective for a variety of aryl iodides/bromides and aryl boronic acids, producing the corresponding biaryl derivatives in good to excellent yields under ambient reaction conditions.

To investigate the industrial application of the designed catalyst, we performed a scale-up synthesis using 5.0 mmol **1a** under the optimized reaction conditions (Scheme 3). The desired cross-coupled product was obtained with a yield of 94%, demonstrating that the developed heterogeneous catalyst is suitable for large-scale synthesis of biaryl derivatives under mild reaction conditions. Furthermore, we sought to explore the reusability of the developed heterogeneous Pd@COF-TFP_TzPy catalyst in SMCC reactions. In this context,

Table 1 Optimization of reaction conditions for the Suzuki–Miyaura cross-coupling reaction[a]

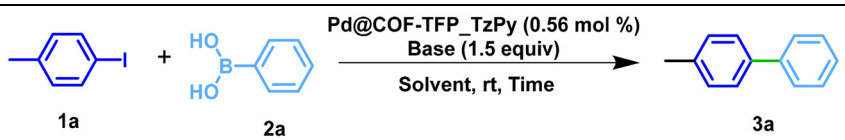

1a 2a 3a

Entry	Catalyst	Solvent	Base	Time (hour)	NMR yield (%)
1	Pd@COF-TFP_TzPy	EtOH : H_2O	K_3PO_4	3	83
2	**Pd@COF-TFP_TzPy**	**EtOH : H_2O**	**NaOH**	**3**	**90**[b]
3	Pd@COF-TFP_TzPy	EtOH : H_2O	K_2CO_3	3	72
4	Pd@COF-TFP_TzPy	EtOH	K_3PO_4	3	58
5	Pd@COF-TFP_TzPy	H_2O	K_3PO_4	24	nr
6	Pd@COF-TFP_TzPy	ACN	K_3PO_4	24	16
7	Pd@COF-TFP_TzPy	DMF : H_2O	K_3PO_4	3	64
8	Pd@COF-TFP_TzPy	ACN : H_2O	K_2CO_3	24	70
9	Pd@COF-TFP_TzPy	Toluene : H_2O	K_3PO_4	24	nr
10	Pd@COF-TFP_TzPy	Toluene	K_3PO_4	24	nr
11	Pd/C	EtOH : H_2O	NaOH	3	62

[a] Reaction conditions: **1a** (0.4 mmol), **2a** (0.6 mmol), a base (0.6 mmol, 1.5 equiv.), and the Pd@COF-TFP_TzPy catalyst (5 mg, 0.5 mol% of Pd@COF-TFP_TzPy catalyst) were stirred in 4 mL of solvent at room temperature. [b] Isolated yield of the product. nr: no reaction.

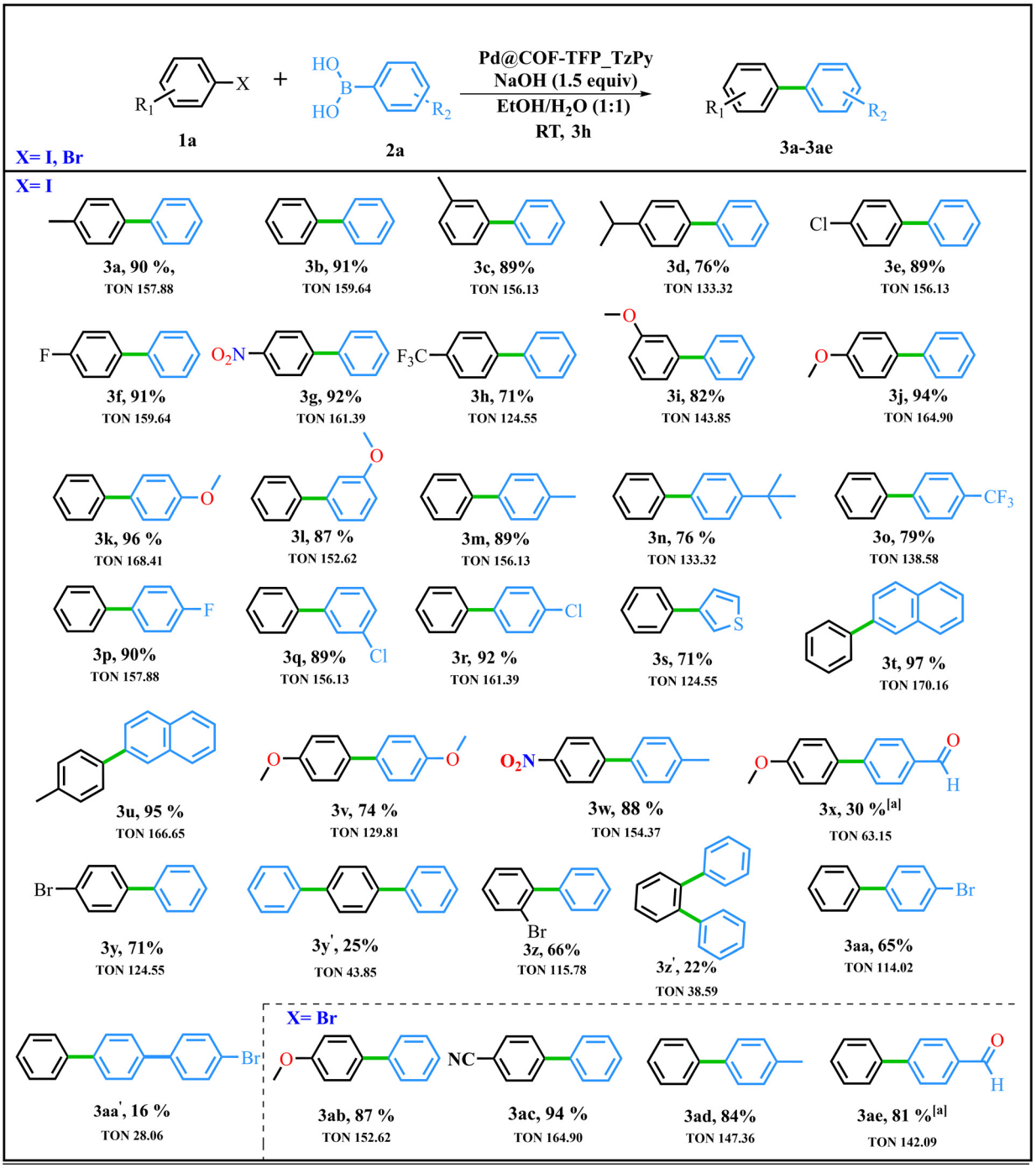

Scheme 2 Substrate scope of SMCC. Reaction conditions: aryl iodide **1a** (0.4 mmol), **2b** (0.6 mmol), NaOH (0.6 mmol), and 5.0 mg (0.56 mol% of Pd@COF-TFP_TzPy) of catalyst were stirred in 4 ml of EtOH/H_2O (1 : 1) for 3 h. [a] Reaction was carried out at 70 °C.

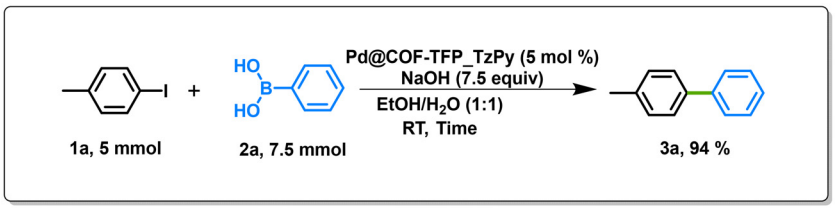

Scheme 3 Scale-up synthesis and reusability test of Pd@COF-TFP_TzPy.

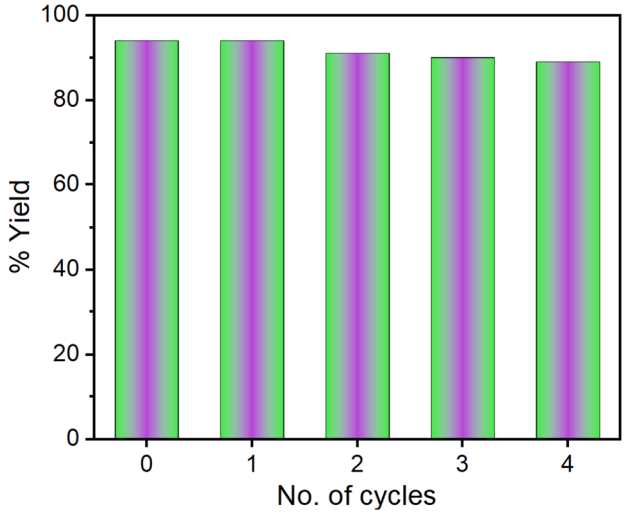

Fig. 6 Reusability of Pd@COF-TFP_TzPy.

the reaction was performed with iodotoluene (**1a**) and phenylboronic acid (**2a**) under optimal conditions (Fig. 6) for five catalytic cycles. After each catalytic cycle, the catalyst was recovered following a standard protocol and reused for subsequent reactions. The results illustrated that the desired biaryl product was consistently isolated in excellent yields (89–94%) even after multiple cycles, highlighting the catalyst's durability and efficiency. We have also provided a plausible mechanistic pathway for the Suzuki–Miyaura coupling (SMC) reaction (Fig. S15†).[59,61]

Motivated by the success of the catalyst for SMCC reactions, we furthermore extended the application of the designed heterogeneous catalyst (Pd@COF-TFP_TzPy) to other popular cross coupling reactions such as Heck and Sonogashira coupling reactions to assess its versatility. Impressive results were observed under the Heck cross coupling reaction conditions. For instance, the reaction of aryl iodide (**4**) with unactivated or activated olefins (**5**) in the presence of triethylamine as a base

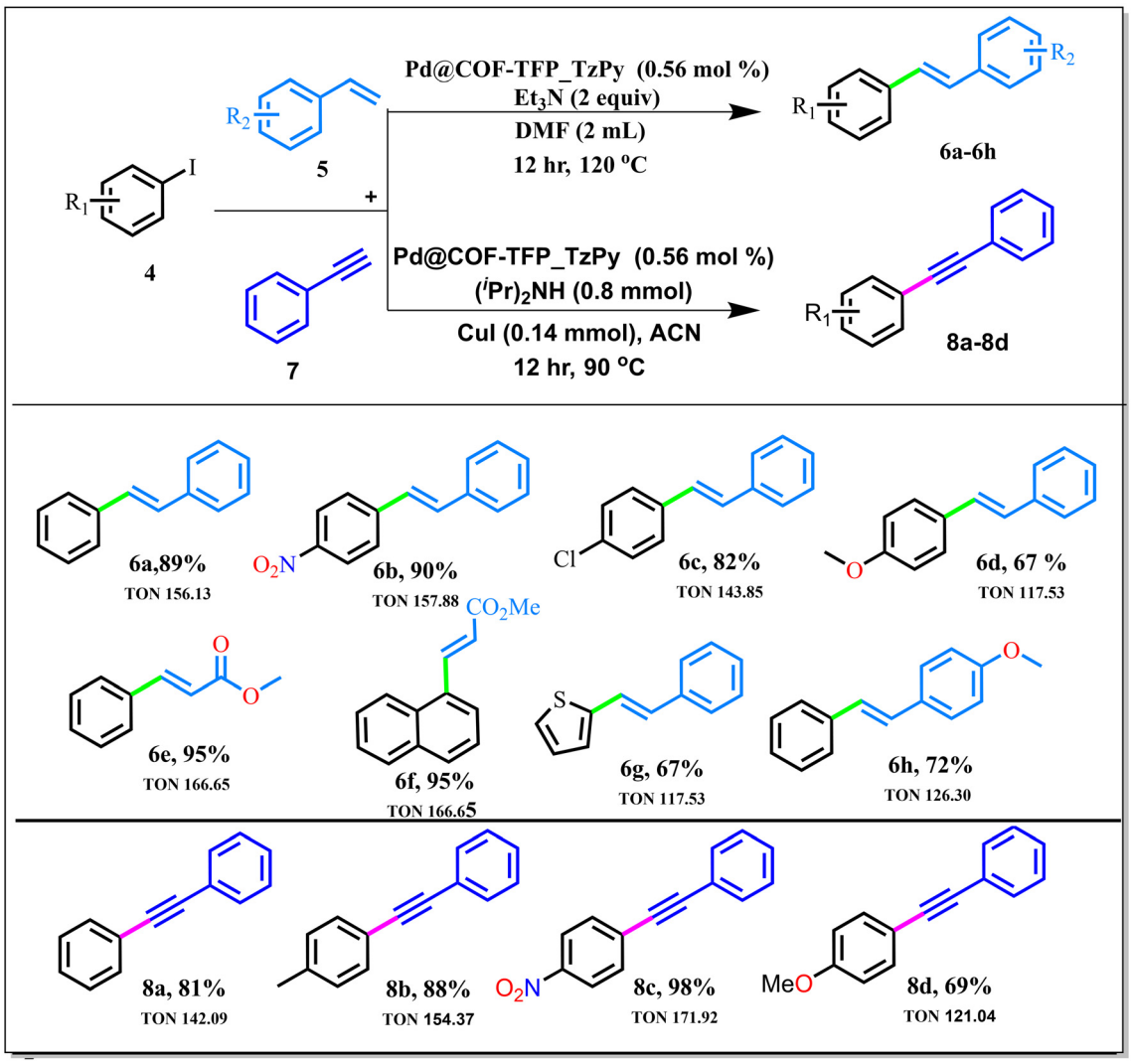

Scheme 4 Substrate scope of Heck and Sonogashira coupling. Reaction conditions: aryl iodide **4** (0.4 mmol), **5** (0.8 mmol), Et_3N (0.8 mmol), and 5.0 mg (0.56 mol% of Pd@COF-TFP_TzPy) of catalyst were stirred in 2 ml of DMF for 12 h. Aryl iodide **4** (0.4 mmol), **8** (0.6 mmol), $^{i}Pr_2NH$ (0.8 mmol), CuI (0.14 mmol), and 5.0 mg (0.56 mol% of Pd@COF-TFP_TzPy) of catalyst were stirred in 4 ml of ACN for 12 h.

and Pd@COF-TFP_TzPy as the catalyst in 2.0 ml of DMF at 120 °C gave the desired *E*-olefins in good to excellent yields. Under the optimized reaction conditions, electrically varied aryl iodides (**4**) coupled with styrene to yield the corresponding products in good to high yields (Scheme 4, **6a–6d**, 67–90%). Additionally, reactions of iodobenzene and 1-iodonaphthalene with methyl acrylate produced methyl cinnamate (**6e**, 95%) and methyl (*E*)-3-(naphthalen-1-yl)acrylate (**6f**, 95%), respectively, highlighting the catalyst's broad applicability. Furthermore, the heterocyclic compound 2-iodothiophene also reacted effectively under the optimized conditions to provide the Heck cross coupled product (**6g**) in 67% yield. Also, iodobenzene reacted with electron-rich styrene to yield the expected product (**6h**) in 72% yield. Notably, the catalyst works effectively for the synthesis of valuable internal alkyne synthons in good to excellent yields under modified Sonogashira cross coupling reaction conditions (Scheme 4. **8a–8d**, 69–98%).

The recyclability of the COF catalyst was thoroughly evaluated after carrying out the coupling reactions. The recovered catalyst was characterized by FT-IR, P-XRD, XPS and N_2 gas adsorption to confirm its stability under optimized reaction conditions. FT-IR analysis showed no deviation in the characteristic stretching frequencies relative to the parent catalyst (Fig. S14a†). Notably, the post-catalysis P-XRD patterns (Fig. S14b†) showed no significant changes in the P-XRD patterns compared to the fresh catalyst. In addition, the retention of permanent porosity in the spent catalyst was confirmed by N_2 gas adsorption studies (Fig. 14c†). XPS analysis further confirmed that Pd remained in the +2 oxidation state, with Pd $3d_5/_2$ and Pd $3d_3/_2$, respectively, indicating the absence of metallic Pd(0) particles even after multiple catalytic cycles (Fig. S 14d†).

Conclusion

In summary, we describe an imine-functionalized covalent organic framework (COF-TFP_TzPy) that was obtained using readily available monomers and a simple synthetic approach. COF-TFP_TzPy is decorated with ample heterocycles (such as 1,3,5-triazine and pyridine units) in the polymeric framework that provide multiple metal coordination units. Thus, COF-TFP_TzPy was reacted with $Pd(OAc)_2$ to incorporate Pd(II) units in the polymeric framework that was confirmed by spectroscopic analyses. The resulting metalated COF (Pd@COF-TFP_TzPy) was tested as a heterogeneous catalyst for cross-coupling reactions, which are crucial for forming carbon–carbon bonds. Pd@COF-TFP_TzPy demonstrated exceptional catalytic performance that was characterized by a broad range of reactants, excellent product yields, high stability, and easy recyclability. Compared to other crystalline porous materials like zeolites and metal–organic frameworks (MOFs), the unique structure of Pd@COF-TFP_TzPy allows efficient substrate access to catalytic sites and rapid mass transport of reactants and products, which in turn contribute to its superior catalytic activity (for a detailed comparison see Table T1, ESI†). We believe that our approach will stimulate further research into functional COF materials for catalysis, potentially leading to their industrial applications.

Author contributions

Atikur Hassan and Neeladri Das conceived and designed the research work. Atikur Hassan, Sk Abdul Wahed and Subhadip Mondal synthesized and characterized the COFs under the supervision of Neeladri Das. Ayush Kumar carried out the catalytic studies under the supervision of Amit Kumar. All authors reviewed and approved the final version of the manuscript.

Data availability

All the additional data are available in the ESI.†

Conflicts of interest

The authors declare no conflict of interest.

Acknowledgements

The authors thank the Indian Institute of Technology (IIT) Patna and CSIR, New Delhi (02(0435)/21/EMR-II) for financial support. Atikur Hassan, Ayush Kumar, and Sk Abdul Wahed thank IIT Patna for an Institute Research Fellowship. The authors also acknowledge SAIF-IIT Patna for providing the NMR facilities. The authors are also grateful to SAIF IIT Bombay for providing the ICP-AES facility. The authors are grateful to RRCAT, Indore, for providing the XPS facility.

References

1 M. Busch, M. D. Wodrich and C. Corminboeuf, *ACS Catal.*, 2017, **7**, 5643–5653.
2 V. P. Mehta and E. V. Van der Eycken, *Chem. Soc. Rev.*, 2011, **40**, 4925–4936.
3 A. Srivastava, H. Kaur, H. Pahuja, T. M. Rangarajan, R. S. Varma and S. Pasricha, *Coord. Chem. Rev.*, 2024, **507**, 215763.
4 J. Struwe, L. Ackermann and F. Gallou, *Chem. Catal.*, 2023, **3**, 100485.
5 A. Hassan, A. S. Baghel, A. Kumar and N. Das, *Chem. – Asian J.*, 2024, **19**, e202300778.
6 Á. Mastalir and Á. Molnár, *Coord. Chem. Rev.*, 2022, **470**, 214696.
7 M. Koy, P. Bellotti, M. Das and F. Glorius, *Nat. Catal.*, 2021, **4**, 352–363.
8 A. Dhakshinamoorthy, A. M. Asiri and H. Garcia, *ACS Catal.*, 2019, **9**, 1081–1102.

9 Z. Chen, E. Vorobyeva, S. Mitchell, E. Fako, M. A. Ortuño, N. López, S. M. Collins, P. A. Midgley, S. Richard, G. Vilé and J. Pérez-Ramírez, *Nat. Nanotechnol.*, 2018, **13**, 702–707.
10 M. Pagliaro, V. Pandarus, R. Ciriminna, F. Béland and P. Demma Carà, *ChemCatChem*, 2012, **4**, 432–445.
11 Y. Zhi, Z. Wang, H.-L. Zhang and Q. Zhang, *Small*, 2020, **16**, 2001070.
12 Á. Mastalir and Á. Molnár, *ChemCatChem*, 2023, **15**, e202300643.
13 A. M. Trzeciak and A. W. Augustyniak, *Coord. Chem. Rev.*, 2019, **384**, 1–20.
14 S. McCarthy, D. C. Braddock and J. D. E. T. Wilton-Ely, *Coord. Chem. Rev.*, 2021, **442**, 213925.
15 N. Esteban, M. L. Ferrer, C. O. Ania, J. G. de la Campa, Á. E. Lozano, C. Álvarez and J. A. Miguel, *ACS Appl. Mater. Interfaces*, 2020, **12**, 56974–56986.
16 D. Astruc, F. Lu and J. R. Aranzaes, *Angew. Chem., Int. Ed.*, 2005, **44**, 7852–7872.
17 M. O. Ivanytsya, V. V. Subotin, K. S. Gavrilenko, S. V. Ryabukhin, D. M. Volochnyuk and S. V. Kolotilov, *Chem. Rec.*, 2024, **24**, e202300300.
18 V. Polshettiwar, C. Len and A. Fihri, *Coord. Chem. Rev.*, 2009, **253**, 2599–2626.
19 J. Guo and D. Jiang, *ACS Cent. Sci.*, 2020, **6**, 869–879.
20 H.-Y. Cheng and T. Wang, *Adv. Synth. Catal.*, 2021, **363**, 144–193.
21 H. Hu, Q. Yan, R. Ge and Y. Gao, *Chin. J. Catal.*, 2018, **39**, 1167–1179.
22 G. Collins, M. Schmidt, C. O'Dwyer, G. McGlacken and J. D. Holmes, *ACS Catal.*, 2014, **4**, 3105–3111.
23 S. Guo, Y. Wu, S.-X. L. Luo and T. M. Swager, *ACS Appl. Nano Mater.*, 2022, **5**, 18603–18611.
24 P. J. Waller, F. Gándara and O. M. Yaghi, *Acc. Chem. Res.*, 2015, **48**, 3053–3063.
25 Y. Jin, Y. Hu and W. Zhang, *Nat. Rev. Chem.*, 2017, **1**, 0056.
26 Y. Song, Q. Sun, B. Aguila and S. Ma, *Adv. Sci.*, 2019, **6**, 1801410.
27 A. Basak, S. Karak and R. Banerjee, *J. Am. Chem. Soc.*, 2023, **145**, 7592–7599.
28 A. Jati, K. Dey, M. Nurhuda, M. A. Addicoat, R. Banerjee and B. Maji, *J. Am. Chem. Soc.*, 2022, **144**, 7822–7833.
29 M. Traxler, S. Gisbertz, P. Pachfule, J. Schmidt, J. Roeser, S. Reischauer, J. Rabeah, B. Pieber and A. Thomas, *Angew. Chem., Int. Ed.*, 2022, **61**, e202117738.
30 S. Dutta, J. I. Hernández García, B. Mishra, D. D. Díaz and P. Pachfule, *Cryst. Growth Des.*, 2024, **24**, 6081–6094.
31 A. Alam, B. Kumbhakar, A. Chakraborty, B. Mishra, S. Ghosh, A. Thomas and P. Pachfule, *ACS Mater. Lett.*, 2024, **6**, 2007–2049.
32 K. Prakash, B. Mishra, D. D. Díaz, C. M. Nagaraja and P. Pachfule, *J. Mater. Chem. A*, 2023, **11**, 14489–14538.
33 Q. Guan, L.-L. Zhou and Y.-B. Dong, *Chem. Soc. Rev.*, 2022, **51**, 6307–6416.
34 A. Hassan, S. A. Wahed, S. Goswami, S. Mondal and N. Das, *ACS Appl. Nano Mater.*, 2024, **7**, 16413–16421.
35 A. Hassan, M. M. R. Mollah, S. Das and N. Das, *J. Mater. Chem. A*, 2023, **11**, 17226–17236.
36 A. Hassan, S. Roy, A. Das, S. A. Wahed, A. Bairagi, S. Mondal, N. Chatterjee and N. Das, *ACS Biomater. Sci. Eng.*, 2024, **10**, 4227–4236.
37 S. Nayak, A. Hassan, N. Das and P. Das, *Chem. Commun.*, 2023, **59**, 8548–8551.
38 T. Huang, W. Zhang, S. Yang, L. Wang and G. Yu, *SmartMat*, 2024, **5**, e1309.
39 S.-Y. Ding and W. Wang, *Chem. Soc. Rev.*, 2013, **42**, 548–568.
40 S.-Y. Ding, J. Gao, Q. Wang, Y. Zhang, W.-G. Song, C.-Y. Su and W. Wang, *J. Am. Chem. Soc.*, 2011, **133**, 19816–19822.
41 C. S. Diercks and O. M. Yaghi, *Science*, 2017, **355**, eaal1585.
42 S. J. Lyle, P. J. Waller and O. M. Yaghi, *Trends Chem.*, 2019, **1**, 172–184.
43 X. Feng, X. Ding and D. Jiang, *Chem. Soc. Rev.*, 2012, **41**, 6010–6022.
44 S. Abednatanzi, M. Najafi, P. Gohari Derakhshandeh and P. Van Der Voort, *Coord. Chem. Rev.*, 2022, **451**, 214259.
45 X. Kan, J.-C. Wang and Y.-B. Dong, *Chem. Commun.*, 2024, **60**, 6362–6374.
46 A. Chakraborty, M. Roy, A. Alam, D. Adhikari and P. Pachfule, *Green Chem.*, 2024, **26**, 9619–9651.
47 S. S. A. Shah, M. S. Javed, T. Najam, M. A. Nazir, A. ur Rehman, A. Rauf, M. Sohail, F. Verpoort and S.-J. Bao, *Mater. Today*, 2023, **67**, 229–255.
48 Y. Hou, X. Zhang, J. Sun, S. Lin, D. Qi, R. Hong, D. Li, X. Xiao and J. Jiang, *Microporous Mesoporous Mater.*, 2015, **214**, 108–114.
49 Y. Yusran, H. Li, X. Guan, Q. Fang and S. Qiu, *EnergyChem*, 2020, **2**, 100035.
50 P. M. Heintz, B. P. Schumacher, M. Chen, W. Huang and L. M. Stanley, *ChemCatChem*, 2019, **11**, 4286–4290.
51 A. Hassan, A. Alam, M. Ansari and N. Das, *Chem. Eng. J.*, 2022, **427**, 130950.
52 S. Haldar, R. Kushwaha, R. Maity and R. Vaidhyanathan, *ACS Mater. Lett.*, 2019, **1**, 490–497.
53 S. Fajal, D. Majumder, W. Mandal, S. Let, G. K. Dam, M. M. Shirolkar and S. K. Ghosh, *J. Mater. Chem. A*, 2023, **11**, 26580–26591.
54 L. Căta, N. Terenti, C. Cociug, N. D. Hădade, I. Grosu, C. Bucur, B. Cojocaru, V. I. Parvulescu, M. Mazur and J. Čejka, *ACS Appl. Mater. Interfaces*, 2022, **14**, 10428–10437.
55 S. Let, G. K. Dam, P. Samanta, S. Fajal, S. Dutta and S. K. Ghosh, *J. Org. Chem.*, 2022, **87**, 16655–16664.
56 H.-C. Ma, J.-L. Kan, G.-J. Chen, C.-X. Chen and Y.-B. Dong, *Chem. Mater.*, 2017, **29**, 6518–6524.
57 R. S. B. Gonçalves, A. B. V. de Oliveira, H. C. Sindra, B. S. Archanjo, M. E. Mendoza, L. S. A. Carneiro, C. D. Buarque and P. M. Esteves, *ChemCatChem*, 2016, **8**, 743–750.
58 D. Saha, R. Sen, T. Maity and S. Koner, *Langmuir*, 2013, **29**, 3140–3151.
59 P. Das and W. Linert, *Coord. Chem. Rev.*, 2016, **311**, 1–23.
60 R. Malav and S. Ray, *Inorg. Chim. Acta*, 2023, **551**, 121478.
61 T. Chen, Y. Pang, S. H. Ali, L. Chen, Y. Li, X. Yan and B. Wang, *Mol. Catal.*, 2024, **558**, 114045.